

The early diagnostic value of optical coherence tomography (OCT) and OCT angiography in thyroid-associated ophthalmopathy

Bei Xu , Sha Wang, Lu Chen and Jia Tan

Abstract

Background: The retinal microvascular density changes have been identified in thyroid-associated ophthalmopathy (TAO) patients. Whereas a lack of research has been done on the diagnostic ability of optical coherence tomography (OCT) combined with optical coherence tomography angiography (OCTA) parameters.

Objectives: This study aims to evaluate the retina perfusion variations in eyes with active and stable TAO and its diagnostic abilities using OCT and OCTA.

Design: This is cohort longitudinal retrospective study.

Methods: A total of 51 patients with TAO and 39 healthy controls (HCs) were recruited. The TAO eyes were divided into active and stable stage groups. The foveal avascular zone (FAZ), macular perfusion density (mPD), and peripapillary PD were measured by OCTA. The peripapillary retinal nerve fiber layer (RNFL), central retinal thickness (CRT), and whole macular volume (wMV) were measured by OCT. Visual evoked potential (VEP) and visual field (VF) were also assessed.

Results: The mPD of the superficial retinal capillary plexus (SRCP) was significantly different in all subfields among active, stable, and HC groups ($p < 0.05$) except for the temporal inner ($p = 0.137$), and the active group achieved the lowest PD. The FAZ size increased significantly in the active and stable groups compared with the HC group ($p < 0.001$). Significant difference was observed in mPD of deep retinal capillary plexus (DRCP) in all quadrants among three groups ($p < 0.05$). Moreover, PD parameters of optic nerve head (ONH) and radial peripapillary capillary plexus (RPCP) showed a different trend among three groups ($p < 0.05$). The r -value of visual field-mean deviation (VF-MD) of TAO with DRCP-whole PD (wPD) and RPCP-wPD was 0.421 and 0.299, respectively ($p < 0.05$). The DRCP-wPD in OCTA and RNFL in OCT were significantly higher in area under the receiver operating characteristic curve (AUC) than that of HC eyes.

Conclusion: OCT and OCTA can noninvasively detect the peripapillary and macular changes in various stages of TAO patients, and it might be a high diagnostic value tool to monitor the TAO progression.

Keywords: diagnostic value, OCT angiography, optical coherence tomography angiography, perfusion density, thyroid-associated ophthalmopathy

Received: 19 June 2022; revised manuscript accepted: 14 March 2023.

Ther Adv Chronic Dis

2023, Vol. 14: 1–11

DOI: 10.1177/
20406223231166802

© The Author(s), 2023.
Article reuse guidelines:
[sagepub.com/journals-](https://sagepub.com/journals-permissions)
permissions

Correspondence to:

Jia Tan

Eye Center of Xiangya
Hospital, Central South
University, Changsha,
China.

Hunan Key Laboratory
of Ophthalmology,
Central South University,
Changsha, China

National Clinical Research
Center for Geriatric
Disorders, Xiangya
Hospital, Central South
University, Changsha,
China

Department of
Ophthalmology, Xiangya
Hospital, Central South
University, No.87 Xiangya
Road, Changsha 410008,
China.

jasmintj@126.com

**Bei Xu
Sha Wang
Lu Chen**

Eye Center of Xiangya
Hospital, Central South
University, Changsha,
China

Hunan Key Laboratory
of Ophthalmology,
Central South University,
Changsha, China

National Clinical Research
Center for Geriatric
Disorders, Xiangya
Hospital, Central South
University, Changsha,
China

Introduction

Thyroid-associated ophthalmopathy (TAO) is an autoimmune mediated inflammatory disorder and affects orbital tissue. The condition shows in patients with hyperthyroidism, euthyroidism, or hypothyroidism.¹ It shows a range of clinical manifestations, including upper eyelid retraction, eyeball proptosis, cornea exposure, limited eye movement, and apical compression of the optic nerve.² The proliferation of orbital fibroblasts, inflammatory cellular infiltration with plasma cells, lymphocytes, mast cells and macrophages, and the overproduction of glycosaminoglycans and collagen were the pathogenesis features of this disease.³ All these contribute to the expansion of extraocular muscles and intraorbital fat which lead to the increased volume of orbital contents and retrobulbar pressure.^{3,4} It is the leading theory of the severe consequence of compressive optic neuropathy (ON) which requires prompt evaluation and treatment. As early optic nerve variations in clinic are inapparent, it is difficult to detect optic nerve involvement in TAO. Retinal and optic disk structure and function, however, may be acquired alterations before the appearance of the ON;⁵⁻⁷ for earlier detection of ON, previous studies has been reported that latency of P100 in the visual evoked potential (VEP) was an early indicator of ON to prevent visual loss.^{8,9} Moreover, visual field (VF) test, contrast sensitivity test, and color sensation test have been used to evaluate the visual function and prevent irreversible visual-threatening.⁹⁻¹²

Various techniques have been used to evaluate the orbital blood flow of TAO patients. Alimgil *et al.*¹³ revealed that in Graves ophthalmopathy (GO) patients, elevated intraorbital pressure led to the increase in venous pressure and choroidal vessel resistance, and then, ocular blood flow was significantly decreased. As an advanced technique, optical coherence tomography (OCT) and optical coherence tomography angiography (OCTA) enable visualize detailed structure and microvasculature with high-quality retina image. Several studies have evaluated variations of vessel density in TAO patients,¹⁴⁻¹⁶ but obtained conflicting results. In addition, microvasculature changes in the retina and the foveal avascular zone (FAZ) size are considered an indicator of the visual acuity, which facilitates further study of early abnormalities in retina of TAO patients.¹⁷ Meanwhile, perfusion density (PD) focuses on

differentiating the movable and stable structures, which can be used to detect changes in retinal blood vessels at different clinical stages and obtain more timely and accurate retinal circulation flow maps. Besides, the determination of the treatment of diverse clinic stages of TAO may take into account the combining of OCTA and OCT parameters.^{17,18} In this study, we aim to evaluate the retina perfusion variations in eyes with active and stable TAO and its diagnostic abilities using OCT and OCTA and its correlation with the visual function.

Materials and methods

Enrollment of participants

All subjects were recruited from the Department of Ophthalmology at Xiangya Hospital, Central South University from December 2019 to June 2021. A total of 51 random eyes from TAO patients were divided into two groups based on the clinical activity scores (CASs):¹⁹ (1) spontaneous orbital pain, (2) staring induced orbital pain, (3) eyelid swelling, (4) eyelid erythema, (5) conjunctival redness, (6) suppurative necrosis, (7) sarcoma inflammation, or plica. Patients with $CAS \geq 3/7$ were defined as active TAO, and those with $CAS \leq 2/7$ were stable TAO. All patients with TAO were newly diagnosed. At the same time, 39 healthy volunteers of matched age were recruited for physical examination as the control group. According to the design of randomized controlled trial, taking deep retinal capillary plexus-whole perfusion density (DRCP-wPD) as the evaluation index, referring to previous research and presurvey data, the DRCP-wPD of the control group was 0.299, the DRCP-wPD of the disease group was 0.421, and the common standard deviation of the two groups was 0.18. Under the condition of $\alpha=0.05$ and $\beta=0.2$, assuming the homogeneity of variance between the two groups, PASS software was used to calculate 36 cases in each group, which could achieve 80% statistical efficiency. The cases in the control group and the disease group were 39 and 51, respectively, which met the requirements of sample size. Exclusion criteria for patients and healthy participants included (1) thyroid treatment within 3 months, like radioactive iodine therapy, immunosuppressor agents, and thyroid surgery; (2) hormone therapy within 6 months; (3) ophthalmic surgery history; (4) concomitant eye diseases, like

glaucoma, retinal vein occlusion, maculopathy, dysthyroid optic neuropathy (DON), and ON; refractive error [$> \pm 3$ diopters (D) sphere and ± 2 D cylinder]; (5) complicated with infection or severe systemic diseases; systolic blood pressure greater than 150 mmHg or less than 100 mmHg, diastolic blood pressure greater than 90 mmHg or less than 60 mmHg; and (6) decreased visual acuity [the best-corrected visual acuity (BCVA) in logMAR visual chart, > 0.2], apparent VF defect [mean deviation (MD) in Humphrey perimetry, < -10 dB], and apical congestion is evident on orbital CT and magnetic resonance imaging. OCT and OCTA images with the following characteristics were excluded: (1) signal strength index < 7 ; (2) motor artifacts visible on the en face angiogram; (3) local weak signal; and (4) images off-center on fovea or disk.

Ophthalmic and systemic examination

All participants received a complete ophthalmic examination including BCVA, intraocular pressure (IOP) measurement with the Goldmann applanation tonometry, slit-lamp examination, and axial length (AL). The proptosis was determined by the same examiner using the Hertel exophthalmometry. B-scan ultrasonography was used to evaluate the ocular and orbital structure. Perimetry was conducted with the standard 24-2 Swedish Interactive Thresholding Algorithm on the Humphrey Visual Field Analyzer (Carl Zeiss Meditec, Inc., Dublin, CA, USA),²⁰ and visual field-mean deviation (VF-MD) was recorded. Pattern VEP (GT-2008 V-VI; GOTEC, Chongqing, China) was only performed for all TAO subjects.

OCTA and OCT imaging

Retina microvasculature imaging based on the Nidek RS-3000 Advance device (Nidek, Gamagori, Japan)²¹ of all participants was obtained. The PD (total area of perfusion vessels per unit area in the measurement area) of macular and peripapillary data at different retinal layers was recorded. Spectral domain optical coherence tomography (SD-OCT) and OCTA images were collected and analyzed by the updated AngioScan software. The optic nerve head (ONH) and fovea were artificially entered, and each eye was scanned in 6 mm \times 6 mm mode. The PD of macular and peripapillary parameters was measured using the

inbuilt software. Retina was automatically segmented into superficial retinal capillary plexus (SRCP) and deep retinal capillary plexus (DRCP), including center area, inner and outer rings of diameters 6 mm, and the inner and outer rings segmented into four sectors, that is, superior, nasal, inferior, and temporal. Automatic segmentation defines the panel (determined by automatic segmentation) where the SRCP extends 12 μ m below the core layer from the inner limiting membranes. The panel of the DRCP extends from 8 μ m below the inner nuclear layer to 12 μ m below the outer nuclear layer. The retinal thickness and macular perfusion density (mPD) were obtained. Central retinal thickness (CRT) was represented as the average thickness of the 1 mm ring in the center of the retina, whole macular volume (wMV), and peripapillary retinal nerve fiber layer (RNFL) were measured by an automatic analysis algorithm of OCT. For optic nerve OCTA, the PD of radial peripapillary capillary plexus (RPCP) network (located in the RNFL) and ONH layer was imaged, including the superior area and inferior area of diameters 6 mm. The FAZ area was calculated using the manufacturer's angiometric software.

Statistics analysis

SPSS 25.0 was used for statistical analysis. Continuous variables with a normal distribution were represented by mean and standard deviation. The independent samples *t*-test was used to make comparisons between two groups and one-way analysis of variance (ANOVA) (if the variances were equal) and the Brown-Forsythe test (if the variances were not equal) for multiple groups. The median (interquartile range) was used to analyze continuous variables that did not follow a normal distribution. The Wilcoxon rank sum test was recruited to make comparisons between two groups and the Kruskal-Wallis *H* test for multiple groups. Categorical variables were represented as frequencies (percentage), and the chi-square test was employed to make comparisons between multiple groups. Correlation analysis was performed using the Pearson and Spearman correlations. A difference of $p < 0.05$ was considered statistically significant. The area under the receiver operating characteristic curve (AUC) was conducted to evaluate the diagnostic capability of different parameters of OCT and OCTA in TAO.

Results

A total of 90 participants were recruited here, including 39 healthy controls (HCs), 28 active patients, and 23 stable patients. No statistical difference was identified in sex distribution ($p=0.279$), age ($p=0.126$), IOP ($p=0.538$), BCVA ($p=0.242$), CRT ($p=0.160$), and mWV ($p=0.078$) among the active, stable, and HC groups (Table 1). VF-MD and P100 latency were obviously different between the active and stable groups (Table 1, $p < 0.001$). Moreover, proptosis and RNFL showed significant differences among three groups (Table 1, $p < 0.001$), the values of RNFL were lower in stable group than in HC, while it reached the highest in active group.

MPD parameters

The results demonstrated that mPD of the SRCP was significantly different in all subfields except

temporal inner ($p=0.137$) among three groups ($p < 0.05$) (Table 2), the active group obtained the lowest PD. The FAZ size increased significantly in the active and stable groups in comparison with the HC group ($p < 0.001$) (Table 2). Similarly, significant difference was found mPD of DRCP in all quadrants among three groups ($p < 0.05$) (Table 3). Post hoc test revealed that the difference of mPD between the active and stable groups was statistically significant only in DRCP except fovea and temporal inner ($p < 0.05$), active and stable groups significant differs from HC in almost all quadrants of DRCP (Table 3), but only several areas in SRCP (Table 2).

Peripapillary PD parameters

The PD parameters of ONH and RPCP in all grids were significantly different among three groups ($p < 0.05$) (Table 4). The average PD values of the ONH in inferior, superior, and whole

Table 1. Clinical characteristics of all included eyes.

	Active	Stable	HC	p-value	Post hoc analysis p-value		
					Active versus stable	Active versus HC	Stable versus HC
Sex				0.279 ^a			
Male	10 (35.7)	6 (26.1)	18 (46.2)				
Female	18 (64.3)	17 (73.9)	21 (53.8)				
Age (years)	49.61 ± 12.42	44.17 ± 10.89	44.72 ± 9.71	0.126 ^b			
BCVA (logMAR)	0.00 (-0.08-0.05)	0.00 (-0.08-0.15)	0.00 (-0.08-0.00)	0.242 ^c			
IOP (mmHg)	16.54 ± 3.32	16.17 ± 1.44	15.87 ± 2.04	0.538 ^d			
CAS	3.00 (3.00-3.00)	1.00 (0.00-1.50)	-	<0.001 ^e			
PROP (mm)	18.32 ± 3.04	17.24 ± 2.79	14.95 ± 1.32	<0.001 ^d	0.468	<0.001	0.003
VF-MD (dB)	-2.13 ± 0.78	-1.10 ± 0.64	-	<0.001 ^e			
P100 latency (ms)	105.79 ± 2.41	102.87 ± 2.33	-	<0.001 ^e			
RNFL (μm)	114.93 ± 7.58	103.74 ± 8.40	108.03 ± 9.15	<0.001 ^b	<0.001	0.005	0.175
CRT (μm)	241.07 ± 35.83	242.65 ± 13.44	251.64 ± 14.44	0.160 ^d			
wMV (mm ³)	8.50 ± 0.26	8.51 ± 0.30	8.67 ± 0.38	0.078 ^b			

BCVA, best-corrected visual acuity; CAS, clinical activity scores; CRT, central retinal thickness; HC, health control; IOP, intraocular pressure; PROP, proptosis; RNFL, retinal nerve fiber layer; VF-MD, visual field-mean deviation; wMV, whole macular volume.

^aChi-square test.

^bOne-way ANOVA.

^cKruskal-Wallis *H* test.

^dBrown-Forsythe test.

^eIndependent samples *t*-test.

Table 2. Superficial retinal capillary plexus (SRCP) perfusion densities in the active, stable, and HC eyes.

	Active	Stable	HC	<i>p</i> -value	Post hoc analysis <i>p</i> -value		
					Active versus stable	Active versus HC	Stable versus HC
Fovea	17.00 (10.00~19.50)	16.00 (15.00~18.00)	19.00 (16.00~23.00)	0.017 ^b	1.000	0.090	0.031
SI	42.11 ± 6.15	43.61 ± 2.31	46.00 ± 4.39	0.003 ^c	0.555	0.019	0.020
II	43.29 ± 6.05	44.65 ± 3.41	46.74 ± 4.25	0.013 ^a	0.916	0.012	0.285
NI	42.07 ± 5.75	43.04 ± 5.44	46.33 ± 5.58	0.006 ^a	1.000	0.009	0.084
TI	45.64 ± 10.64	46.00 ± 3.44	48.85 ± 4.60	0.137 ^c	–	–	–
SO	48.64 ± 6.68	50.83 ± 3.38	52.74 ± 3.71	0.005 ^c	0.356	0.016	0.121
IO	52.29 ± 4.54	52.35 ± 4.30	54.59 ± 2.12	0.029 ^c	1.000	0.050	0.077
NO	53.43 ± 3.88	53.57 ± 2.79	55.15 ± 2.47	0.042 ^a	1.000	0.075	0.152
TO	45.00 ± 9.35	45.26 ± 5.15	49.13 ± 4.51	0.026 ^c	0.999	0.106	0.014
FAZ	0.37 ± 0.06	0.35 ± 0.03	0.29 ± 0.07	<0.001 ^c	0.216	<0.001	<0.001
SRCP-wPD	43.11 ± 5.36	43.96 ± 1.92	46.57 ± 1.85	0.001 ^c	0.820	0.008	<0.001

FAZ, foveal avascular zone; HC, healthy control; II, inferior inner; IO, inferior outer; NI, nasal inner; NO, nasal outer; SI, superior inner; SO, superior outer; SRCP-wPD, superficial retinal capillary plexus-whole perfusion density; TI, temporal inner; TO, temporal outer.

^aOne-way ANOVA.

^bKruskal–Wallis *H* test.

^cBrown–Forsythe test.

of the active group were lower than those of the stable group without statistically significant difference ($p > 0.05$) (Table 4). PD of the RPCP in inferior and superior has the same tendency with ONH, but the difference between active and stable groups was significant ($p < 0.001$) (Table 4).

Correlation between vessel density and other parameters

The Pearson correlation coefficients and their corresponding *p*-value are presented in Table 5. The *r*-values of VF-MD of TAO patients with DRCP-wPD and RPCP-wPD were 0.421 and 0.299, respectively ($p < 0.05$) (Table 5). CRT was negatively correlated with VF-MD and positively correlated with P100 latency ($p < 0.05$) (Table 5).

Diagnostic abilities of OCTA and OCT

The AUC for distinguishing active and HC eyes in OCTA was the highest for DRCP-wPD (0.998), followed by RPCP-wPD (0.939), FAZ (0.823),

SRCP-wPD (0.755), and ONH-wPD (0.708). In OCT, RNFL was the highest for active/HC (0.731), followed by ONH-wPD (0.708), wMV (0.640), and CRT (0.577). In the pairwise comparison, the DRCP-wPD in OCTA and RNFL in OCT owned a higher AUC than that of differentiating active from HC eyes (Figure 1).

Discussion

A lack of research has been done on the diagnostic ability of OCT combined with OCTA parameters and whether they can serve as early signs of visual loss at different stages of TAO. The retinal microvascular density changes has been identified in TAO patients in previous studies,¹⁵ but the results were inconsistent. In this study, we excluded the patients with elevated systemic pressure, which may cause increased cardiac output and orbital blood flow.²² It might partially explain the discrepancy. In addition, the differences in techniques and disease staging, such as inactive or stable stage, were also factors contributing to

Table 3. Deep retinal capillary plexus (DRCP) perfusion densities in the active, stable, and HC eyes.

	Active	Stable	HC	p-value	Post hoc analysis p-value		
					Active versus stable	Active versus HC	Stable versus HC
DRCP-wPD	28.91 ± 2.53	33.65 ± 3.43	41.25 ± 5.44	<0.001 ^a	<0.001	<0.001	<0.001
Fovea	16.21 ± 3.99	17.48 ± 2.92	19.72 ± 4.82	0.002 ^a	0.480	0.006	0.076
SI	34.96 ± 4.51	41.30 ± 9.18	47.59 ± 8.98	<0.001 ^a	0.015	<0.001	0.034
II	29.36 ± 4.59	36.22 ± 5.97	41.31 ± 8.50	<0.001 ^a	<0.001	<0.001	0.023
NI	36.82 ± 5.19	42.91 ± 8.24	51.54 ± 8.34	<0.001 ^a	0.012	<0.001	0.001
TI	33.86 ± 5.05	36.96 ± 6.26	48.41 ± 8.58	<0.001 ^a	0.173	<0.001	<0.001
SO	26.29 ± 4.43	32.04 ± 3.21	40.15 ± 5.87	<0.001 ^a	<0.001	<0.001	<0.001
IO	21.86 ± 3.60	26.87 ± 4.77	34.95 ± 6.64	<0.001 ^a	<0.001	<0.001	<0.001
NO	30.36 ± 5.62	34.91 ± 4.93	42.95 ± 8.45	<0.001 ^a	0.010	<0.001	<0.001
TO	30.50 ± 5.89	34.17 ± 4.02	44.67 ± 7.25	<0.001 ^a	0.033	<0.001	<0.001

DRCP-wPD, deep retinal capillary plexus-whole perfusion density; HC, healthy control; II, inferior inner; IO, inferior outer; NI, nasal inner; NO, nasal outer; SI, superior inner; SO, superior outer; TI, temporal inner; TO, temporal outer.
^aBrown-Forsythe test.

this difference.¹⁷ Finally, the TAO participants involved in this study were uncomplicated with DON and without any appearance change. We explored the retinal hemodynamic and structure change in TAO patients at active and stable stages according to CAS. Our research studied PD which symbolized the total area of the perfused vasculature per unit area within an OCTA measurement area. In addition, multidepth assessment of retinal perfusion was performed on cross-sectional images. OCTA offers qualitative and quantitative data of the microcirculation and the PD.

We found in OCT and OCTA parameters in Table 2, except for the PD of the temporal inner quadrant in SRCP, the other quadrants were significantly different among three groups. We observed that PD decreased in active TAO patients. Moreover, as revealed from the post hoc analysis p-value, active and stable groups significantly differ from HC in almost all quadrants of DRCP, but only several areas in SRCP. The trend of ONH and RPCP was similar, and the

difference of PD in all fields was significant among groups. But no significant difference was observed in ONH (superior) and ONH (inferior) between stable and HC groups. Retinal perfusion depends mainly upon the orbital blood supply. The Doppler ultrasonography have been used to study the hemodynamic variation and concluded that superior ophthalmic vein had lower flow velocity and stasis in TAO patients.²³ It is known that inflammatory changes recurrent in orbital spaces could lead to chronic atrophic. Then, the orbit compression and macular thinning were found in stable patients.²⁴ Meanwhile, decreased consumption of nutrients and oxygen occurred in atrophic tissue causes lowered blood flow.²³ Compressive ON might be the severe consequence of orbit compression. Besides, orbital fibroblast mediator, stimulated by orbital fibroblasts and turned into adipocytes and fibroblasts, is thought to be an important cause of orbit compression.^{25,26} The compression of orbit puts pressure on the venous system, causing retro blood flow. In addition, the inflammatory changes can increase orbital arterial

Table 4. Optic nerve head (ONH) and radial peripapillary capillary layer (RPCP) densities in the active, stable, and HC eyes.

	Active	Stable	HC	<i>p</i> -value	Post hoc analysis <i>p</i> -value		
					Active versus stable	Active versus HC	Stable versus HC
ONH (S)	44.43 ± 3.52	44.57 ± 2.91	46.38 ± 2.84	0.018 ^a	1.000	0.037	0.082
ONH (I)	43.93 ± 5.25	45.04 ± 2.88	47.03 ± 3.77	0.010 ^b	0.710	0.031	0.069
ONH (WHOLE)	44.18 ± 3.87	44.70 ± 2.33	46.71 ± 2.71	0.002 ^a	1.000	0.004	0.041
RPCP (S)	45.86 ± 2.86	50.91 ± 5.51	52.85 ± 3.60	<0.001 ^b	0.001	<0.001	0.362
RPCP (I)	43.50 ± 3.82	47.52 ± 3.91	51.03 ± 3.98	<0.001 ^a	0.001	<0.001	0.003
RPCP (WHOLE)	44.68 ± 2.74	49.22 ± 4.37	51.94 ± 3.28	<0.001 ^a	<0.001	<0.001	0.040

I, inferior; ONH, optic nerve head; RPCP, radial peripapillary capillary plexus; S, superior.
^aOne-way ANOVA.
^bBrown-Forsythe test.

Table 5. Pearson correlation coefficient matrix on parameters of optical coherence tomography (OCT) and optical coherence tomography angiography (OCTA) and visual functions.

	SRCP-wPD	DRCP-wPD	ONH-wPD	RPCP-wPD	CRT	RNFL	FAZ
VF-MD							
<i>r</i>	0.133	0.421	0.207	0.299	-0.481	-0.034	-0.064
<i>p</i>	0.353	0.002	0.145	0.033	0.000	0.810	0.657
P100 latency							
<i>r</i>	-0.257	-0.183	-0.079	-0.232	0.337	-0.021	0.115
<i>p</i>	0.069	0.199	0.581	0.102	0.016	0.886	0.422
BCVA							
<i>r</i>	-0.125	-0.162	-0.198	-0.059	0.052	-0.065	0.174
<i>p</i>	0.242	0.128	0.062	0.580	0.630	0.545	0.101

BCVA, best-corrected visual acuity; CRT, central retinal thickness; DRCP-wPD, deep retinal capillary plexus-whole perfusion density; FAZ, foveal avascular zone; ONH-wPD, optic nerve head-whole perfusion density; RNFL, peripapillary retinal fiber layer; RPCP-wPD, radial peripapillary capillary plexus-whole perfusion density; SRCP-wPD, superficial retinal capillary plexus-whole perfusion density; VF-MD, visual field-mean deviation.

blood flow velocities.²⁷ Meanwhile, inflammatory variations could cause intraorbital congestion and an increased episcleral venous pressure, and then the central retinal vein is obstructed.²⁸ It is a possible explanation for reduced macular and ONH perfusion in patients compared with HC. The temporal retinal ring is usually the thinnest,

making the difference between HC and affected eyes smaller and therefore hard to detect. Exophthalmos is a result of the expansion of orbital fat and muscle tissue into the bone structure. In this study, the Hertel exophthalmometry values were higher in the active group, but not statistically significant. Marked inflammation was

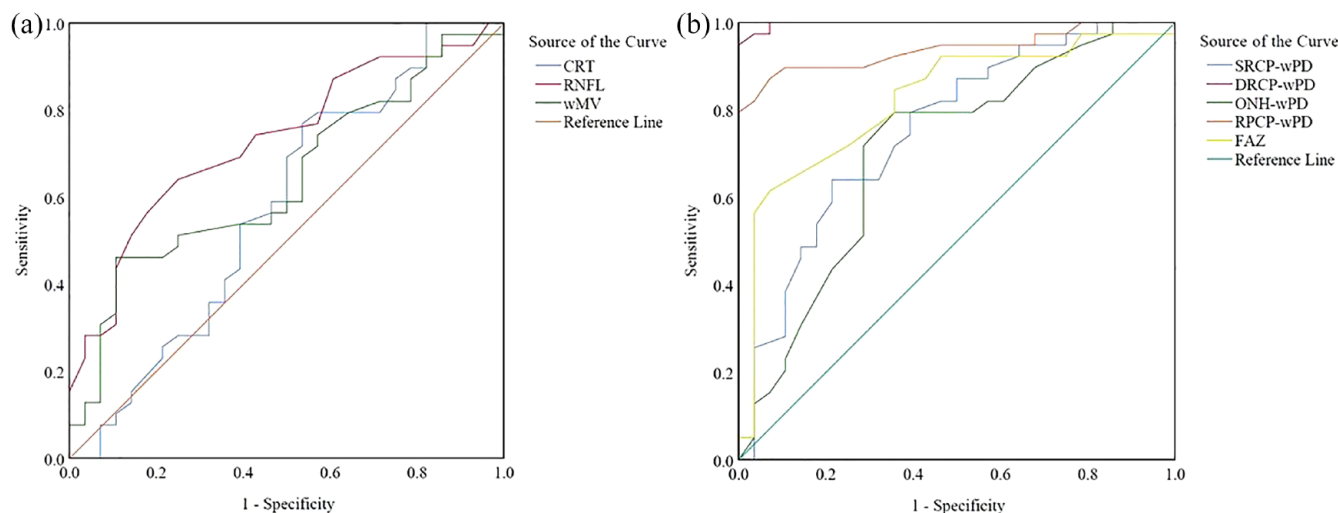


Figure 1. The area under the receiver operator characteristic curves (AUROCs) for differentiating active from healthy controls. (a) Optical coherence tomography (OCT) measurements: CRT thickness (0.577), RNFL thickness (0.731), and wMV (0.640). (b) OCT angiography (OCTA) measurements: SRCP-wPD (0.755), DRCP-wPD (0.998), ONH-wPD (0.708), RPCP-wPD (0.939), and FAZ (0.823).

observed during the active phase, followed by a period of stability. Recurrent inflammatory in inactive patients leads to chronic atrophic changes and macular thinning.

DRCP is a more sensitive and early indicator in our investigation, which could be caused by various factors, like the different circulation systems. Retinal circulation produced in endothelial cells is regulated by local factors and only supplies the SRCP.²⁹ Meanwhile, both the DRCP and macular area are fed by choroidal circulations with less autoregulation, it is known that perfusion pressure and sympathetic innervation are the main factors influencing choroidal blood flow.¹⁷ Chiara Del Noce *et al.*³⁰ found that vascular flow of choriocapillaris was reduced in TAO patients compared with HC, which implied that the decreased PD in DRCP of macular caused by the high congestion of ophthalmic veins reduced choroid drainage. Hence, it is speculated that orbital blood determined the fundus perfusion, and the pathological changes in orbital tissues lead to the perfusion variations in the orbit.

Here, we further found FAZ area enlarged in active TAO patients, and the difference was significant when compared with the HC group. FAZ is the most sensitive in retina and the capillary free zone in central macula. Previous research

demonstrated that FAZ enlargement promoted the appearance of capillary perfusion more objectively.^{21,31}

The thickening of the peripapillary RNFL in active stage is predicted by an elevated retrobulbar pressure-based etiology and an inflammatory process. McKeag *et al.*³² revealed that disk edema appeared in 56% eyes with diagnosed ON, and it was an effective marker for ON. Intro-orbital inflammation and edema may give rise to optic disk swelling in TAO patients.

A normal-looking appearance of optic disk is, however, thought to be the coexistence of optic disk atrophy with axon loss and optic disk swelling and inflammation combined with inflammatory mechanisms and compressive mechanisms. The compression mechanism is found in glaucomatous eyes which finally results in macular thinning and RNFL loss.³³ This is consistent with our OCT results. Therefore, early changes in TAO can be better monitored and understand with the objective parameters of OCT and OCTA.

Furthermore, we also found that DRCP-wPD and RPCP-wPD positively correlated with VF-MD. According to the previous studies, VF-MD defects and VEP were considered as the early sign of DON even in the presence of normal

visual acuity,^{12,34} suggesting that they can be applied to the early assessment of VF changes.

The AUC showed that the DRCP-wPD was of a high value to distinguish the active eyes from HC in OCTA. Combined with the fact that there was no significant difference among three groups in structural parameters (CRT and wMV) in this research, the diagnostic value of OCTA and OCT was confirmed. We inferred the peripapillary and mPD changes might precede structural changes.

Some limitations, however, remained in our research. First, the sample size was small; we can only see the tendency of the parameters reflecting the stage of the disease. In addition, the use of medicine was not considered in TAO patients, which is a biased evaluation of the severity of the disease. Besides, this study was cross-sectional and failed to capture PD changes over time. Finally, further longitudinal and larger sample study should be performed in the following experiment.

Conclusion

In conclusion, the results suggested the peripapillary and mPD changes might precede structural changes. Furthermore, DRCP-wPD and RNFL have a high value in distinguishing the active eyes from HC which confirmed the diagnose value of OCTA and OCT. The PD in DRCP is promising early sign to detect the variations in various stages of TAO more sensitively.

Declarations

Ethics approval and consent to participate

The ethical committee of Xiangya Hospital of Central South University approved this retrospective cohort study, which was performed in the Xiangya Hospital of Central South University. The informed consent was waived due to decoding between the original data sets and personal information listed, as well as approved by the Xiangya Hospital of Central South University (#202112273).

Consent for publication

Not applicable.

Author contributions

Bei Xu: Data curation; Formal analysis; Funding acquisition; Investigation; Resources; Software;

Writing – original draft; Writing – review & editing.

Sha Wang: Data curation; Formal analysis; Investigation; Resources; Visualization; Writing – review & editing.

Lu Chen: Data curation; Formal analysis; Investigation; Methodology; Software; Validation; Visualization; Writing – review & editing.

Jia Tan: Conceptualization; Formal analysis; Funding acquisition; Investigation; Project administration; Resources; Software; Supervision; Validation; Writing – review & editing.

Acknowledgements

The authors acknowledge all authors of the original studies that were included in this study.

Funding

The authors disclosed receipt of the following financial support for the research, authorship, and/or publication of this article: This study was supported by the Natural Science Foundation for Scientists of Hunan Province [China Hunan Provincial Science and Technology Department (grant no. 2022JJ30959)]. The funding body did not have any role in the design of the study, the collection, analysis and interpretation of the data, or the writing of the manuscript.


Competing interests

The authors declared no potential conflicts of interest with respect to the research, authorship, and/or publication of this article.

Availability of data and materials

The data used to support the findings of this study are included within the article. The primary data used to support the findings of this study are available from the corresponding author upon request.

ORCID iD

Bei Xu  <https://orcid.org/0000-0002-9701-7014>

References

1. Bartley GB. The epidemiologic characteristics and clinical course of ophthalmopathy associated with autoimmune thyroid disease in Olmsted County, Minnesota. *Trans Am Ophthalmol Soc* 1994; 92: 477–588.

2. Dolman PJ. Grading severity and activity in thyroid eye disease. *Ophthalmic Plast Reconstr Surg* 2018; 34(Suppl. 1): S34–S40.
3. McAlinden C. An overview of thyroid eye disease. *Eye Vis* 2014; 1: 9.
4. Maheshwari R and Weis E. Thyroid associated orbitopathy. *Indian J Ophthalmol* 2012; 60: 87–93.
5. Beden Ü, Kaya S, Yeter V, *et al.* Contrast sensitivity of thyroid associated ophthalmopathy patients without obvious optic neuropathy. *ScientificWorldJournal* 2013; 2013: 943789.
6. Hallin ES, Feldon SE and Luttrell J. Graves' ophthalmopathy: III. Effect of transantral orbital decompression on optic neuropathy. *Br J Ophthalmol* 1988; 72: 683–687.
7. Kennerdell JS, Rosenbaum AE and El-Hoshy MH. Apical optic nerve compression of dysthyroid optic neuropathy on computed tomography. *Arch Ophthalmol* 1981; 99: 807–809.
8. Iao TWU, Rong SS, Ling AN, *et al.* Electrophysiological studies in thyroid associated orbitopathy: a systematic review. *Sci Rep* 2017; 7: 12108.
9. Pérez-Rico C, Rodríguez-González N, Arévalo-Serrano J, *et al.* Evaluation of multifocal visual evoked potentials in patients with Graves' orbitopathy and subclinical optic nerve involvement. *Doc Ophthalmol* 2012; 125: 11–19.
10. Eckstein A, Dekowski D, Führer-Sakel D, *et al.* Graves' ophthalmopathy. *Ophthalmologe* 2016; 113: 349–364. Quiz 465–346.
11. Sen E, Berker D, Elgin U, *et al.* Comparison of optic disc topography in the cases with Graves disease and healthy controls. *J Glaucoma* 2012; 21: 586–589.
12. Neigel JM, Rootman J, Belkin RI, *et al.* Dysthyroid optic neuropathy. The crowded orbital apex syndrome. *Ophthalmology* 1988; 95: 1515–1521.
13. Alimgil ML, Benian O, Esgin H, *et al.* Ocular pulse amplitude in patients with Graves' disease: a preliminary study. *Acta Ophthalmol Scand* 1999; 77: 694–696.
14. Qian GF, Yuan LS, Chen M, *et al.* PPWD1 is associated with the occurrence of postmenopausal osteoporosis as determined by weighted gene co-expression network analysis. *Mol Med Rep* 2019; 20: 3202–3214.
15. Ye L, Zhou SS, Yang WL, *et al.* Retinal microvasculature alteration in active thyroid-associated ophthalmopathy. *Endocr Pract* 2018; 24: 658–667.
16. Akpolat C, Kurt MM, Yılmaz M, *et al.* Analysis of foveal and parafoveal microvascular density and retinal vessel caliber alteration in inactive Graves' ophthalmopathy. *J Ophthalmol* 2020; 2020: 7643737.
17. Perri P, Campa C, Costagliola C, *et al.* Increased retinal blood flow in patients with active Graves' ophthalmopathy. *Curr Eye Res* 2007; 32: 985–990.
18. Çalışkan S, Acar M and Gürdal C. Choroidal thickness in patients with Graves' ophthalmopathy. *Curr Eye Res* 2017; 42: 484–490.
19. Bartalena L, Baldeschi L, Dickinson AJ, *et al.* Consensus statement of the European Group on Graves' Orbitopathy (EUGOGO) on management of Graves' orbitopathy. *Thyroid* 2008; 18: 333–346.
20. Rangaswamy NV, Patel HM, Locke KG, *et al.* A comparison of visual field sensitivity to photoreceptor thickness in retinitis pigmentosa. *Invest Ophthalmol Vis Sci* 2010; 51: 4213–4219.
21. Yılmaz H, Karakurt Y, Icel E, *et al.* Normative data assessment of vessel density and foveal avascular zone metrics using AngioScan software. *Curr Eye Res* 2019; 44: 1345–1352.
22. Mercé J, Ferrás S, Oltra C, *et al.* Cardiovascular abnormalities in hyperthyroidism: a prospective Doppler echocardiographic study. *Am J Med* 2005; 118: 126–131.
23. Monteiro MLR, Angotti-Neto H, Benabou JE, *et al.* Color Doppler imaging of the superior ophthalmic vein in different clinical forms of Graves' orbitopathy. *Jpn J Ophthalmol* 2008; 52: 483–488.
24. Konieczka K, Flammer AJ, Todorova M, *et al.* Retinitis pigmentosa and ocular blood flow. *Epma J* 2012; 3: 17.
25. Bahn RS. Graves' ophthalmopathy. *N Engl J Med* 2010; 362: 726–738.
26. Dik WA, Virakul S and van Steensel L. Current perspectives on the role of orbital fibroblasts in the pathogenesis of Graves' ophthalmopathy. *Exp Eye Res* 2016; 142: 83–91.
27. Hiromatsu Y, Yang D, Bednarczuk T, *et al.* Cytokine profiles in eye muscle tissue and orbital fat tissue from patients with thyroid-associated ophthalmopathy. *J Clin Endocrinol Metab* 2000; 85: 1194–1199.
28. Thyparampil P and Yen MT. Compressive optic neuropathy in thyroid eye disease. *Int Ophthalmol Clin* 2016; 56: 51–67.

29. Paques M, Garmyn V, Catier A, *et al.* Analysis of retinal and choroidal circulation during central retinal vein occlusion using indocyanine green videoangiography. *Arch Ophthalmol* 2001; 119: 1781–1787.
30. Del Noce C, Vagge A, Nicolò M, *et al.* Evaluation of choroidal thickness and choroidal vascular blood flow in patients with thyroid-associated orbitopathy (TAO) using SD-OCT and Angio-OCT. *Graefes Arch Clin Exp Ophthalmol* 2020; 258: 1103–1107.
31. Konuk O, Onaran Z, Ozhan Otkar S, *et al.* Intraocular pressure and superior ophthalmic vein blood flow velocity in Graves' orbitopathy: relation with the clinical features. *Graefes Arch Clin Exp Ophthalmol* 2009; 247: 1555–1559.
32. McKeag D, Lane C, Lazarus JH, *et al.* Clinical features of dysthyroid optic neuropathy: a European Group on Graves' Orbitopathy (EUGOGO) survey. *Br J Ophthalmol* 2007; 91: 455–458.
33. Greenfield DS, Bagga H and Knighton RW. Macular thickness changes in glaucomatous optic neuropathy detected using optical coherence tomography. *Arch Ophthalmol* 2003; 121: 41–46.
34. Gasser P and Flammer J. Optic neuropathy of Graves' disease. A report of a perimetric follow-up. *Ophthalmologica* 1986; 192: 22–27.

Visit SAGE journals online
[journals.sagepub.com/
home/taj](http://journals.sagepub.com/home/taj)

 SAGE journals